ISSN: 1983 7402 São José dos Campos, 28 de setembro a 01 de outubro de 2010

New Electro-optic Modulator Highly Insensitive to Temperature

[1,2]William Fegadolli, [1,2]Vilson Rosa Almeida, [1]Olympio Lucchini Coutinho, and [1]José Edimar Barbosa Oliveira
[1]Instituto Tecnológico de Aeronáutica – ITA, Departamento de Microondas e Optoeletrônica
[2]Instituto de Estudos Avançados – IEAv, Divisão de Fotônica
São José dos Campos - SP, Brazil
fegadoli@ita.br

Abstract — **A novel compact silicon electro-optic modulator is theoretically proposed and analyzed. The device is designed to be entirely compatible with CMOS process. Numerical simulation results show that a compact device enables operation over an ultra-broad bandwidth, up to 865 GHz; moreover and most importantly, the device is highly insensitive to temperature variations, up to 75 K**

Keywords-component; Modulators; Integrated optics devices; Coupled waveguides

I. INTRODUCTION

Silicon photonics has been considered a very promising technology for present and future applications due to its potential applicability to low-cost high-bandwidth telecommunication applications down to the chip level [1, 2]. One of the greatest advantages of this technology is the strong optical confinement achieved in high index contrast optical systems [1], as well as a well established fabrication technology that is easily integrated with CMOS systems [2]. During the last few years, several active and passive devices have been proposed, such as: electro-optic modulators [3], optical filters [4], electro-optic switches [5], optical reflectors [6], tunable lasers [7], all-optical switches [8], and all-optical modulators [9], besides many others.

Although several silicon photonics devices have been proposed and analyzed, there are several challenges that still need to be overcome by science and technology. One of the greatest, perhaps the most relevant weakness of silicon photonics, is its high sensitivity to temperature [10]; typical silicon photonic devices are highly sensitive to temperature as a direct consequence of the large silicon thermo-optical coefficient [10].

Some researchers have presented suggestions on how to solve this problem. A typical solution presented has been the utilization of a polymer with negative thermo-optical coefficient in order to compensate the temperature effect [11, 12]; however, that solution is not very practical, because it makes the device lose one of its most important potential advantages, the capability of integration with CMOS technology, due to the incompatibility between CMOS and polymers.

Therefore, a long-standing challenge in silicon photonics has been the pursuit of developing, by means of intrinsic design, a device which is insensitive to temperature over a large range; additionally, it is of foremost importance that such device designed presents a compact footprint and allows for compatibility with CMOS technology. In this paper, an innovative approach for an electro-optic modulator is theoretically presented and analyzed, the proposed device is based on a coupled ring resonator structure; such device is herein called "Snowman Modulator" due to its obvious physical similarity.

This paper is organized as follow: in the second section, the proposed device is mathematically analyzed and depicted; in the third section, the obtained analytical and numerical results are presented; finally, some considerations and conclusions are presented.

II. THEORETICAL ANALYSIS OF THE DEVICE

The proposed device is schematically shown in Fig. 1, consisting of two coupled ring resonators, which in turn are coupled to a bus waveguide. In this paper, this coupled ring resonator structure was analyzed by means of scattering parameters; it is noteworthy to point out that several authors have shown the efficiency of this analytical tool by means of the concordance of Finite-Difference Time-Domain – FDTD method and experimental results [5, 6, 13, 14, 15].

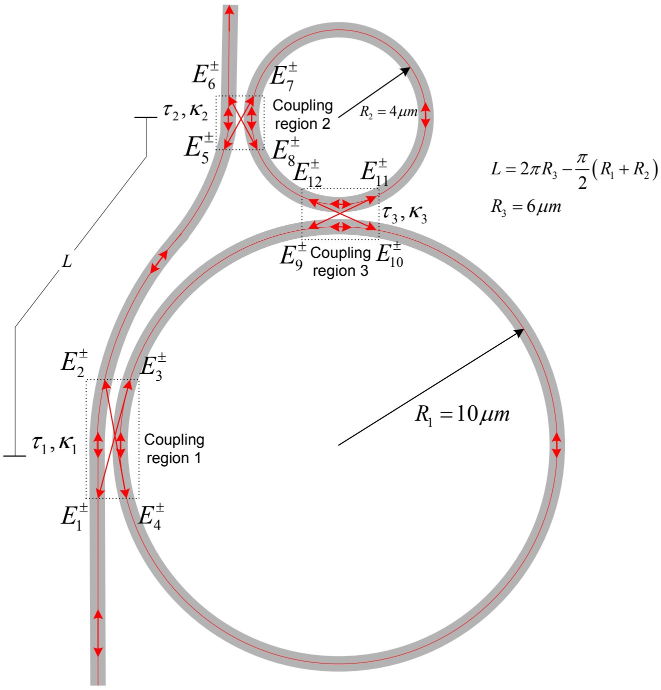

Fig. 1: Schematic representation of a Snowman Modulator

One can notice three distinct coupling regions, which are appropriately labeled, in Fig.1; each coupling region is a directional coupler, which can be modeled as a four-port optical device. The symbol E_i^+ corresponds to the *i*-th input electric field, representing the optical beam fed into the respective port, whereas E_i^- relates to the *i*-th output electric field counterpart for the respective port.

The scattering matrix which describes the output electric field components as a function of the input electric field (E_{in}) is described by (1), where τ_1 and κ_1 are, respectively, the transmission and the coupling coefficient between the major ring resonator and the bus waveguide; τ_2 and κ_2 are, respectively, the transmission and the coupling coefficient between the minor ring resonator and the bus waveguide; τ_3 and κ_3 are, respectively, the transmission and the coupling coefficient between the two ring resonators. ϕ_1, ϕ_2, and ϕ_3 are the optical phases accumulated due to propagation inside ring resonator 1, ring resonator 2, and length L, respectively; ϕ_1, ϕ_2, and ϕ_3 are given by:

$$\phi_1 = \frac{2\pi}{\lambda_0} n_{eff} \left(2\pi R_1\right), \tag{2}$$

$$\phi_2 = \frac{2\pi}{\lambda_0} n_{eff} \left(2\pi R_2\right), \tag{3}$$

$$\phi_3 = \frac{2\pi}{\lambda_0} n_{eff} L \ , \tag{4}$$

where λ_0 is the free space wavelength and n_{eff} is the complex effective index of refraction for ring resonators and waveguides. R_1 is the radius of the major ring resonator, R_2 is the radius of the minor ring resonator, L is the length of the waveguide which connects the coupled resonators.

Among the set of coupled equations specified by means of (1), special attention is given to E_6^- and E_1^-, because these electric fields are the ones that describe the optical response of the device, *i.e.*, they are the electric field components that leave the device; thereby, its optical response can be assessed analyzing the optical intensity at output ports 1 and 6. The transmitted and reflected optical intensity responses can be evaluated, respectively, by $I_t(\lambda_0) = |E_6^-/E_{in}|^2$ and $I_r(\lambda_0) = |E_1^-/E_{in}|^2$.

III. THEORETICAL RESULTS OF THE SNOWMAN MODULATOR

Perhaps the greatest advantage of the proposed device is that its optical response can be tailored as a function of the design parameters, *i.e.*, τ_1, τ_2, τ_3, κ_1, κ_2, κ_3, R_1, R_2, L, neglecting the optical losses. Each combination of parameters produces a different optical response, what makes the device be a complex device due its multivariable nature. The proposed configuration is hereby analyzed considering the set of variables shown in Table I, which were chosen amongst typical values found in the literature for ring resonators, as well as an appropriately chosen value for L in order to attain the desirable optical response.

Table I. Variables used at the project of the Snowman Modulator

τ_1	τ_2	τ_3	R_1	R_1	L	α
0.6652	0.9299	0.4972	10 µm	4 µm	5π µm	50 m^{-1}

The directional couplers are considered lossless in this model; therefore, the coupling coefficients are related to the transmission coefficients by means of a simple equation which describes the principle of conservation of energy: $\kappa_i = (1-\tau_i^2)^{1/2}$, where $i = 1, 2, 3$.

The principle of operation consists of modifying the effective index of refraction of the device on an unbalanced way, what can be done, for instance, by means of free carrier injection [16]. In this model, we consider an unbalanced modulation such as the one schematically shown in Fig. 2, which helps illustrate both situations, modulated and not modulated; we considered Δn_{eff} = -0.00365 inside the major ring resonator, Δn_{eff} = -0.00165 inside the minor ring resonator, and Δn_{eff} = -0.00165 in the waveguide of length L.

$$\begin{bmatrix}
1 & 0 & 0 & 0 & -\tau_1 e^{j\phi_3} & 0 & 0 & 0 & j\kappa_1 e^{j\phi_1/4} & 0 & 0 & 0 \\
0 & 1 & 0 & 0 & 0 & 0 & 0 & 0 & 0 & j\kappa_1 e^{-j3\phi_1/4} & 0 & 0 \\
0 & 0 & 1 & 0 & 0 & 0 & 0 & 0 & 0 & -\tau_1 e^{-j3\phi_1/4} & 0 & 0 \\
0 & 0 & 0 & 1 & j\kappa_1 e^{j\phi_3} & 0 & 0 & 0 & -\tau_1 e^{j\phi_1/4} & 0 & 0 & 0 \\
0 & 0 & 0 & 0 & 1 & 0 & 0 & 0 & 0 & 0 & j\kappa_2 e^{j3\phi_2/4} & 0 \\
0 & -\tau_2 e^{-j\phi_3} & 0 & 0 & 0 & 1 & 0 & 0 & 0 & 0 & 0 & j\kappa_2 e^{-j\phi_2/4} \\
0 & j\kappa_2 e^{-j\phi_3} & 0 & 0 & 0 & 0 & 1 & 0 & 0 & 0 & 0 & -\tau_2 e^{j\phi_2/4} \\
0 & 0 & 0 & 0 & 0 & 0 & 0 & 1 & 0 & 0 & -\tau_2 e^{j3\phi_2/4} & 0 \\
0 & 0 & 0 & -\tau_3 e^{j3\phi_1/4} & 0 & 0 & j\kappa_3 e^{-j3\phi_2/4} & 0 & 1 & 0 & 0 & 0 \\
0 & 0 & -\tau_3 e^{-j\phi_1/4} & 0 & 0 & 0 & 0 & j\kappa_3 e^{j\phi_2/4} & 0 & 1 & 0 & 0 \\
0 & 0 & j\kappa_3 e^{-j\phi_1/4} & 0 & 0 & 0 & 0 & -\tau_3 e^{j\phi_2/4} & 0 & 0 & 1 & 0 \\
0 & 0 & 0 & j\kappa_3 e^{j3\phi_1/4} & 0 & 0 & -\tau_3 e^{-j3\phi_2/4} & 0 & 0 & 0 & 0 & 1
\end{bmatrix}
\begin{bmatrix} E_1^- \\ E_2^- \\ E_3^- \\ E_4^- \\ E_5^- \\ E_6^- \\ E_7^- \\ E_8^- \\ E_9^- \\ E_{10}^- \\ E_{11}^- \\ E_{12}^- \end{bmatrix}
=
\begin{bmatrix} 0 \\ \tau_1 E_{in} \\ -j\kappa_1 E_{in} \\ 0 \\ 0 \\ 0 \\ 0 \\ 0 \\ 0 \\ 0 \\ 0 \\ 0 \end{bmatrix} \tag{1}$$

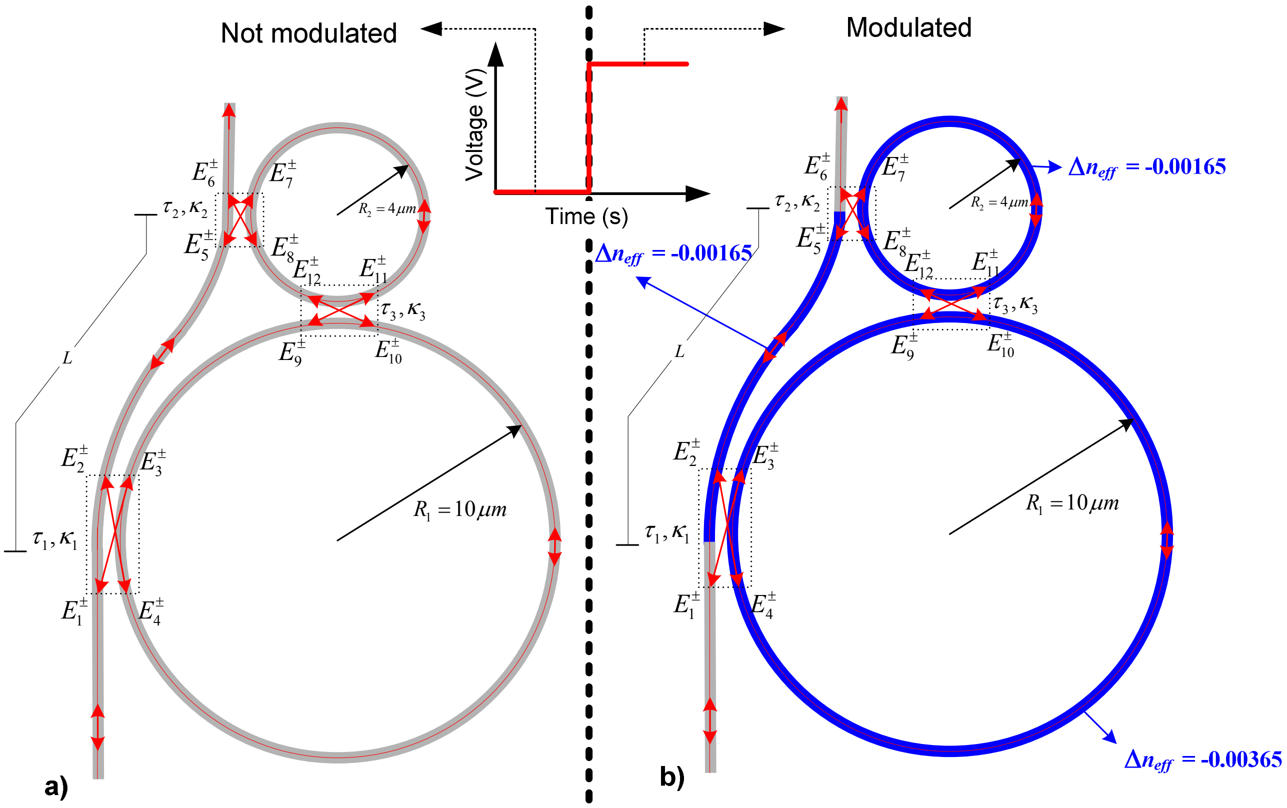

Fig. 2: Schematic representation of a Snowman Modulator: (a) not modulated, (b) modulated

Fig. 3 shows the normalized output intensity as a function of the wavelength, when the Snowman Modulator is considered operating in two stages: modulated and not modulated. In Fig. 3, we considered a waveguide with cross section 400 nm wide and 200 nm thin, as well as the optical losses due to free carrier injection [16]; moreover, the polarization mode is the quasi-TM_{00}.

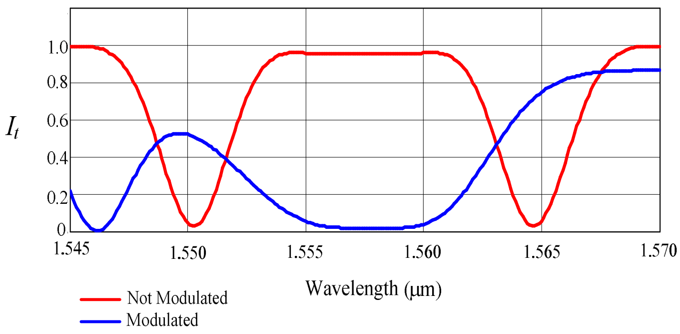

Fig. 3: Normalized transmitted optical intensity response of the Snowman Modulator.

An important observation should be made regarding Fig. 3, where the optical response is only considered for quasi-TM_{00} polarization mode, and the values shown in Table I. If the quasi-TE_{00} polarization was considered, the shape of the optical response would be the same but the wavelength of operation would be slightly different. It occurs due to the distinct optical phase accumulated in each polarization state, which are directly related to the respective effective index of refraction

One can notice the high operation bandwidth of the device. In order to quantify the bandwidth of the device, we analyzed the extinction ratio of the modulator (*i.e.*, the ratio between transmission intensity in both cases) as a function of the wavelength; this result is shown in Fig. 4.

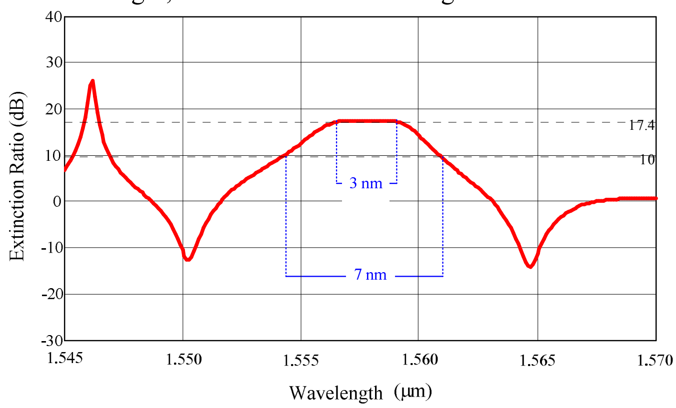

Fig. 4: Extinction ratio for the Snowman Modulator as a function of wavelength

One can observe the high and flat bandwidth of operation of the device, which is approximately of 3 nm, approximately 370 GHz in frequency span, for an extinction ratio of 17 dB or higher. On the other hand, if the minimum extinction ratio can be tolerated to be of 10 dB, one can obtain a bandwidth as wide as 7 nm, which is approximately 865 GHz in frequency span.

This result shows that this proposed compact structure can be used as a broadband modulator or as a broadband switch; nonetheless, a more important characteristic of the proposed device is its intrinsic property of very low temperature sensitivity.

The temperature dependence of the effective index of refraction for silicon waveguides is one of the most critical characteristics that affect the overall optical response of such devices; this dependency varies with several parameters, such as: waveguide dimensions, optical polarization, and wavelength of operation.

The thermo-optical coefficient for silicon and silica are approximately $dn_{Si}/dT = 1.86 \times 10^{-4} K^{-1}$ and $dn_{SiO2}/dT = 1.28 \times 10^{-5} K^{-1}$, respectively; therefore, the effective waveguide thermo-optical coefficient is highly affected by the level of optical confinement, and thus depends directly on the several parameters mentioned above. Therefore, considering a waveguide 400 nm wide and 200nm thin and both polarization states, quasi-TM_{00} and quasi-TE_{00}, its effective thermo-optical coefficient is given by $0.9 \times 10^{-4} K^{-1}$ and $1.8 \times 10^{-4} K^{-1}$, respectively [11,12].

Fig. 5 shows the extinction ratio as a function of the temperature variation, for both polarization states at a wavelength of operation corresponding to the resonance center.

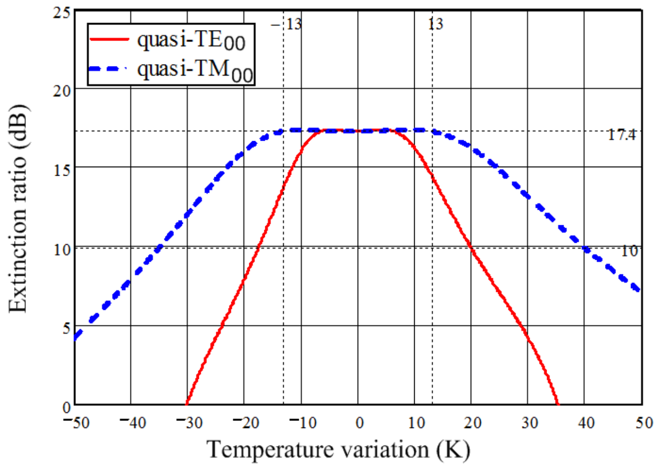

Fig. 5: Extinction ratio a function of temperature variation

One can notice that the temperature sensitivity for the quasi-TE_{00} polarization is twice that for the quasi-TM_{00} counterpart; this occurs due to the different effective thermo-optical coefficient, as mentioned. One can observe in Fig. 5 that the device performance remain completely unaltered under temperature variation of up to 26 K, for quasi-TM_{00}, considering an extinction ratio of approximately 17 dB. Moreover, if an extinction ratio of 10 dB can be tolerated, the device supports up to 75 K of temperature variation.

On the other hand, if the quasi-TE_{00} polarization is chosen, this sensitivity is reduced to half of the previous one, *i.e.*, 13 K for an extinction ratio of 17 dB, and 38 K for an extinction ratio of 10 dB.

IV. Conclusion and Discussion

Based on the results shown in the preview sections, one can classify the silicon Snowman Modulator as a promising integrated optical device, due to its characteristics of ultra-broadband operation, up to 865 GHz, and very low sensitivity to temperature, of up to 75 K when it is tuned to the central resonance wavelength for the quasi-TM_{00}, not to mention its intrinsic characteristics of compactness and CMOS-compatibility.

Therefore, the proposed device may open the door for novel structural configurations of silicon optical devices that are capable of mitigating one of the few remaining sources of criticism for widespread use of silicon photonics – the temperature sensitivity.

References

1. L. Pavesi and G. Guillot, "Optical Interconnects - the silicon approach", Springer-Verlag, Heidelberg, 2006
2. M. L. Calvo and V. Lakshminarayanan, Optical Waveguides: From Theory to Applied Technologies, CRC Press; 1 edition (2007)
3. Q. Xu, B. Schmidt, S. Pradhan, and M. Lipson, "Micrometer-scale silicon electro-optic modulator," Nature 435, 325-327 (2005).
4. Biswajeet Guha, Bernardo B. C. Kyotoku, and Michal Lipson, "CMOS-compatible athermal silicon microring resonators," Opt. Express 18, 3487-3493 (2010)
5. Sang-Yeon Cho and Richard Soref, "Interferometric microring-resonant 2 x 2 optical switches," Opt. Express 16, 13304-13314 (2008)
6. Youngchul Chung, Doo-Gun Kim, and Nadir Dagli, "Reflection Properties of Coupled-Ring Reflectors," J. Lightwave Technol. 24, 1865- (2006)
7. Xuan Wang, Tao Liu, Vilson R. de Almeida, and Roberto R. Panepucci, "On-chip silicon photonic wavelength control of optical fiber lasers," Opt. Express 16, 15671-15676 (2008)
8. Sheng Lan and Hiroshi Ishikawa, "High-efficiency reflection-type all-optical switch for ultrashort pulses based on a single asymmetrically confined photonic crystal defect," Opt. Lett. 27, 1259-1261 (2002)
9. V. R. Almeida, Q. Xu, and M. Lipson, "Ultrafast integrated semiconductor optical modulator based on the plasma-dispersion effect", Optics Letters, v. 30, n. 18, pp. 2403-2405 (2005)
10. B. Frey, D. Leviton, and T. Madison, "Temperature-dependent refractive index of silicon and germanium," Proc. SPIE 6273, 62732J (2006).
11. Jie Teng, Pieter Dumon, Wim Bogaerts, Hongbo Zhang, Xigao Jian, Xiuyou Han, Mingshan Zhao, Geert Morthier, and Roel Baets, "Athermal Silicon-on-insulator ring resonators by overlaying a polymer cladding on narrowed waveguides," Opt. Express 17, 14627-14633 (2009).
12. Jong-Moo Lee, Duk-Jun Kim, Hokyun Ahn, Sang-Ho Park, and Gyungock Kim, "Temperature Dependence of Silicon Nanophotonic Ring Resonator With a Polymeric Overlayer," J. Lightwave Technol. 25, 2236-2243 (2007)
13. Chremmos, I.; Uzunoglu, N., "Reflective properties of double-ring resonator system coupled to a waveguide," Photonics Technology Letters, IEEE , vol.17, no.10, pp. 2110-2112, Oct. 2005.
14. S. Choi, Z. Peng, Q. Yang, E. H. Hwang, and P. D. Dapkus, " A Semiconductor Tunable Laser Using a Wavelength Selective Reflector Based on Ring Resonators," in Optical Fiber Communication Conference and Exposition and The National Fiber Optic Engineers Conference, Technical Digest (CD) (Optical Society of America, 2005), paper PDP20.
15. J.K.S. Poon; J. Scheuer; A. Yariv, "Wavelength-selective reflector based on a circular array of coupled microring resonators," Photonics Technology Letters, IEEE , vol.16, no.5, pp.1331-1333, May 2004.
16. R. A. Soref and B. R. Bennett, "Electrooptical Effects in Silicon," IEEE J. Quantum Electron. 23(1), 123–129 (1987)